Environmental Processes (2018) 5:879–894
https://doi.org/10.1007/s40710-018-0337-0

ORIGINAL ARTICLE

Quantum Dot Size Effect on the Frontier Molecular Orbital Energies in the Presence of Different Aquatic Environmental Ligands

Bianca-Maria Bresolin[1] · Walter Z. Tang[2] · Mika Sillanpää[1,2]

Received: 13 February 2018 / Accepted: 11 October 2018 / Published online: 19 November 2018

Abstract
One of the challenging tasks of the century is to clean up the contaminants of the environment by ecofriendly, sustainable and economically adoptable technologies. The application of quantum dots (QDs) is growing rapidly in to the field of nanotechnology. The electronic properties such as the energy of the highest occupied molecular orbital (E_{HOMO}), the lowest unoccupied molecular orbital (E_{LUMO}), the energy gap ΔE are correlated to the size of quantum dots (QDs) such as CdSe in the presence of different ligands. Linear regression equations were developed through statistical analysis using SPSS. In terms of correlation coefficient R^2, both the size and nature of organic ligand capping affect the E_{HOMO}, E_{LUMO} and ΔE levels of QDs. Among all QDs, CdSe has the strongest correlation between its frontier molecular orbital energy levels with the QDs size. The R^2 value is greater than 0.63 for a regression equation with a coefficient value of −0.17 and a constant of 2.9. This result implies that a unit decrease of size in the range lower than 7 nm would increase the band gap ΔE by 17%. Potential environmental applications of QDs are presented.

Keywords Quantum dots · EHOMO · ELUMO · ΔE · Bandgap · Ligands

1 Introduction

Nanoparticles that show unique size-dependent optical and electrical properties are referred to as quantum dots (QDs) due to their quantum confinement. Reed (1986) was the first who defined the term "quantum dot" in describing ~250 nm molecules, which were then named "spatially quantized system" within which carriers have "zero degree of freedom". "Colloidal" quantum

✉ Bianca-Maria Bresolin
biancabresolin@yahoo.it; bianca-maria.bresolin@lut.fi

[1] Laboratory of Green Chemistry, School of Engineering Science, Lappeenranta University of Technology, Sammonkatu 12, FI-50130 Mikkeli, Finland

[2] Department of Civil and Environmental Engineering, Florida International University, Miami FL-33174, USA

dots produced by wet chemical synthesis were prepared by as zero-dimensional material (Steigerwald and Brus 1989). Currently, the terms "colloidal quantum dot" and "colloidal semiconductor nanocrystal" are used interchangeably. The intricacies of QDs electronic structure depend upon the size and shape of the nanocrystal as well as the band structure of the corresponding bulk material (Klimov 2007, 2014; Nozik et al. 2010; Carey et al. 2015). By alternating the size of nanoparticles and ligand in the solution, the contributions of nanoparticle size and ligand to the energy of the highest occupied molecular orbital (E_{HOMO}), the lowest unoccupied molecular orbital (E_{LUMO}), and the energy gap ΔE could be systematically determined. As a result, photo-voltage, driving forces, and spectral response of highly efficient donor-linker-acceptor components could be optimized (Hagberg et al. 2007). For example, Cui et al. (2001) studied the interaction of QDs with proximate organic molecules present in solution. These ligands influence the electronic and vibrational states of the QDs, the energy of the electron donor transfer and the structural components of QDs assemblies. Moreover, the ligands participate productively in photo-physical processes that make QDs so attractive for many applications in specific photocatalytic reactions. Photo-redox catalysis of QDs is related to the combination of the electronic structure and environment at the surface because QDs catalysts both influence the energy levels of the QDs excited state and drive chemical reactions (Harris et al. 2016). For all these processes, one of the most important variables is the QDs size to tune the electronic property such as the QD E_{HOMO}, E_{LUMO}, and the ΔE between the E_{HOMO} and the E_{LUMO}. Therefore, the relationship between these electronic properties and the QDs diameter, d (nm), is quantified to predict the selectivity of photo-catalysis. ΔE is an important descriptor for the excited state property of organic molecules and usually directly affects their excited state reactions. Quantum mechanical coupling of the QDs, the E_{HOMO} and the E_{LUMO} controls the Raman intensity, thus the optically excited electrons in the metal (Brus 2008). The amplitude of the energy gap of the frontier orbitals, ΔE, is a way to rationally control electron transport properties between molecules (Yoshizawa 2012). Modifications to this interface can change the potential barrier in both the height and the shape of the wave functions. Therefore, they will affect the tunnelling of the electron and hole wave functions into the interfacial region (Harris et al. 2016).

The unique electrical, catalytic, magnetic, mechanical, photonic, and thermal properties of QDs results in their wide applications in industry, agriculture, business, medicine, clothing, cosmetics, and food in the twenty-first century (Oberdörster et al. 2005; Gonzalez et al. 2008; Schmalhofer et al. 2008; Yin et al. 2009), especially in environmental applications. Applications for soil, groundwater, wastewater, air remediation are some of the issues where the ability of nanotechnology to minimize pollution is in progress and could represent revolutionary changes in the environmental field (Bovea et al. 2010; Smith and Nie 2010; Crane and Scott 2012; Zhang et al. 2013). Wastewater remediation using engineered nanoparticles is one of the field among the various applications of the nanotechnology where QDs are more applied (Yadav et al. 2017; Smith and Nie 2010). Thus, the optimization in the synthesis of QDs to control morphologies and sizes must be considered fundamental. Moreover, it is also necessary to develop new methods to assess better understanding of QDs based innovation (Zhang 1997; Burda et al. 2005).

Among the quantum dots under intensive investigation, CdSe stands out as a promising candidate in different applications with its particle size as a determining factor on its optical band gap. Its unique tuneable optical, magnetic, and chemical features are widely used not only in medicine, where they improve the diagnosis, imaging, and treatment of disease but also in water treatment (Liou et al. 1996; Dahan et al. 2003; Alivisatos et al. 2005; Mahmoodi et al. 2016). To improve QDs efficiency, organic ligand phase-transfer process may modify QDs from their hydrophobic state to hydrophilic state (Yu et al. 2007).

Therefore, the main objectives of the current study are: 1) to develop a database of electronic properties such as E_{HOMO}, E_{LUMO}, and ΔE for different QDs of semiconductors and ligands; 2) to conduct regression analysis between E_{HOMO}, E_{LUMO}, and ΔE with the diameter of QDs and interpret the meaning of these regression equations; 3) to validate the correlation equations using other independent data set which was not used in regression analysis; and 4) to quantify the uncertainty of the predicted values by the prediction equations and the experimental data.

2 Material and Methods

2.1 Theory

The exciton wave function is the product of that for electron and hole of QDs, as follows:

$$\Psi_{exc} = \Psi_e \Psi_h \tag{1}$$

where Ψ_{exc}, Ψ_e and Ψ_h are the exciton, the single-electron and single-hole wave functions, respectively.

When the states of the QDs are close to the bulk conduction and valence band edges near $k = 0$, the effective mass/envelope function approximation (EMA/EFA) could be used for the electron and hole wavefunctions:

$$\Psi_e(k, r) = \mu_{CB}(k)\ \Psi_e(r) \tag{2}$$

$$\Psi_h(k, r) = \mu_{CB}(k)\ \Psi_h(r) \tag{3}$$

where the bloch wavefunctions of the conduction band $\mu_{CB}(k)$ and valence band $\mu_{CB}(k)$ have been separated from the electron $\Psi_e(r)$ and hole $\Psi_h(r)$ envelope wavefunctions. The envelope wavefunctions can be calculated by solving the Schrödinger equation ($H\Psi = E\Psi$). Considering the spherically symmetric wavefunctions for a particle-in-a-box, it is possible to simplify the equation by ignoring the radial and angular dependencies θ and ϕ. Therefore, the following treatment would be accurate for the confinement energy of a quantum dot band-edge exciton (EBEE), which represents the difference between the bulk energy gap and the lowest energy optical transition. The BEE state of $1S_{3/2} - 1S_e$ is S-like but will not be accurate for non-S-like states such as the $1PS_{3/2} - 1P_e$. If the electron of a QDs particle is considered as a particle-in-a-box, the Hamiltonian can be written as a sum of the kinetic energy, confinement potential and Coulomb potential:

$$V_{conf,e} = \frac{V_{\infty,e}}{1 + e^{-(r-R)/s}} \tag{4}$$

$$V_{conf,h} = \frac{V_{\infty,h}}{1 + e^{-(r-R)/s}} \tag{5}$$

where: $V_{\infty,e}$ and $V_{\infty,h}$ are the potentials outside the quantum dot for the electron or the hole, respectively; R is the quantum dot size; and s is the softness factor, whose magnitude is directly proportional to how rapidly (in terms of length) the confinement potential changes as the variable r approaches the dot radius R radiating outward from the center of the QDs. Very small values of s would most closely resemble a particle-in-a-box potential.

2.2 Database Description and Statistical Analysis

The data were collected from different peer reviewed research papers to evaluate the energy level of different kinds of QDs in the presence of different organic capping ligands. The data collected were analyzed using *SPSS* Regression Models™ to establish the correlation between independent and dependent factors. The size of QDs is the independent variable in all cases studied. Different dependent factors were taken into account: E_{HOMO}, E_{LUMO}, ΔE. Energy data were regressed using linear models to obtain the slope and the correlation coefficients. The linear equation used is as follows:

$$y = kd + C \tag{6}$$

where: y is the dependent variable, such as E_{HOMO}, E_{LUMO} and ΔE; d is the independent variable (size in nm); k is the slope of the straight line and C is the constant.

The regression equations are reported and discussed in terms of their correlation coefficients and slopes. The regression equations were evaluated and compared. The k value, as slope of the equation line, determines through the sign the concordance or discordance of the variation of the variables; moreover, the higher is the value of k, the higher is the influence of the size on the dependent variable. The constant C, according to other parameters, can be an indicator of the dependent variable level at the lower values of size; thus, it can judge the similarity between the different kinds of particles used or between the ligands. The model was further confirmed by using of *MATLAB* (matrix laboratory) as multi-paradigm numerical computing environment. The residues, as differences between the observed value and the estimated value were evaluated. The equations are presented in graphs to compare the different parameters obtained by the different QDs and ligands used in the experiments.

3 Results and Discussion

Figure 1 describes statistics on QDs size found in Table 1. Figure 2 analyzes E_{HOMO} level frequencies found in Table 2. Frequency analysis was performed to detect if the datasets could

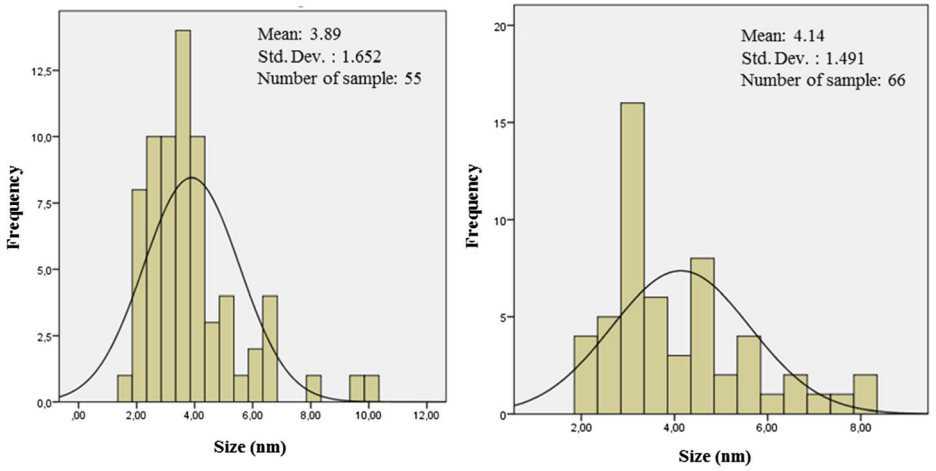

Fig. 1 Histograms of QDs size distribution of two different sets of databases: **a** Table 1; **b**) Table 2

Table 1 E_{HOMO} and QD size

QDs	Capping ligand	Size, nm	HOMO, eV	Reference
CdSe	TOPO	2.10	5.54	(Jasieniak et al. 2011)
	TOPO	2.20	5.65	(Jasieniak et al. 2011)
	TOPO	2.60	5.59	(Jasieniak et al. 2011)
	TOPO	3.20	5.43	(Jasieniak et al. 2011)
	TOPO	4.00	5.44	(Jasieniak et al. 2011)
	TOPO	5.10	5.44	(Jasieniak et al. 2011)
	TOPO	5.70	5.37	(Jasieniak et al. 2011)
	TOPO	6.40	5.38	(Jasieniak et al. 2011)
	TOPO	2.70	5.80	(Ehamparam et al. 2015)
	alkylamines	4.70	5.40	(Ehamparam et al. 2015)
	TOPO	4.70	5.45	(Jasieniak et al. 2011)
	oleate	4.70	5.60	(Jasieniak et al. 2011)
	alkanethiols	4.70	5.65	(Jasieniak et al. 2011)
	pyridine	4.70	5.75	(Jasieniak et al. 2011)
	1-hexanthiol	3.60	6.20	(Munro et al. 2010)
	1-benzenethiol	3.60	6.30	(Munro et al. 2010)
	1-fluorothiophenol	3.60	6.30	(Munro et al. 2010)
CdTe	TOPO	2.30	5.00	(Jasieniak et al. 2011)
	TOPO	2.50	5.07	(Jasieniak et al. 2011)
	TOPO	3.30	4.99	(Jasieniak et al. 2011)
	TOPO	3.60	4.96	(Jasieniak et al. 2011)
	TOPO	3.90	4.89	(Jasieniak et al. 2011)
	TOPO	4.60	4.86	(Jasieniak et al. 2011)
	TOPO	5.10	4.87	(Jasieniak et al. 2011)
	TOPO	5.60	4.91	(Jasieniak et al. 2011)
PbS	oleate	2.80	5.02	(Jasieniak et al. 2011)
	oleate	3.30	4.99	(Jasieniak et al. 2011)
	oleate	3.70	5.02	(Jasieniak et al. 2011)
	oleate	3.90	4.96	(Jasieniak et al. 2011)
	oleate	4.50	4.95	(Jasieniak et al. 2011)
	oleate	5.40	4.89	(Jasieniak et al. 2011)
	oleate	6.10	4.89	(Jasieniak et al. 2011)
	oleate	7.20	4.87	(Jasieniak et al. 2011)
	oleate	8.10	4.81	(Jasieniak et al. 2011)
	TBABr	3.30	5.90	(Brown et al. 2014)
	TBAI	3.30	5.80	(Brown et al. 2014)
	TBACl	3.30	5.70	(Brown et al. 2014)
	NH4SCN	3.30	5.60	(Brown et al. 2014)
	1,4-benzendithiol	3.30	5.50	(Brown et al. 2014)
	1,3-benzenedithiol	3.30	5.40	(Brown et al. 2014)
	1,2-benzenedithiol	3.30	5.27	(Brown et al. 2014)
	TBAF	3.30	5.25	(Brown et al. 2014)
	ethanedithiol	3.30	5.20	(Brown et al. 2014)
	1-mercaptopropionic	3.30	5.10	(Brown et al. 2014)
	1,2-ethylenediamine	3.30	5.10	(Brown et al. 2014)
	thiophenol	3.30	4.90	(Brown et al. 2014)
PbSe	oleate	2.10	5.01	(Jasieniak et al. 2011)
	oleate	2.60	5.02	(Jasieniak et al. 2011)
	oleate	3.30	4.96	(Jasieniak et al. 2011)
	oleate	3.60	4.88	(Jasieniak et al. 2011)
	oleate	4.40	4.86	(Jasieniak et al. 2011)
	oleate	5.40	4.87	(Jasieniak et al. 2011)
	oleate	6.40	4.91	(Jasieniak et al. 2011)
	oleate	7.60	4.83	(Jasieniak et al. 2011)
	oleate	8.30	4.85	(Jasieniak et al. 2011)

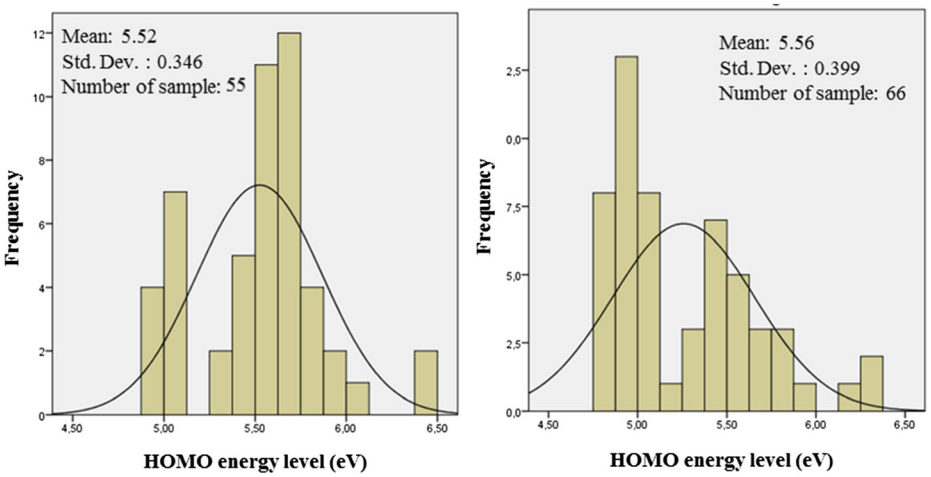

Fig. 2 E_{HOMO} (eV) frequencies distribution of two different sets of databases: **a** Table 1; **b**) Table 2

be compared. Figure 1a depicts the histogram plot of distribution of different QDs size at different diameters (nm) related to Table 1 dataset. The QDs size spreads from 2 to 8 nm. The majority of available data belong to particles with 3.9 nm size as indicated by the mean value with a standard deviation of 1.65 nm. The second dataset (Table 2) is analysed in Fig. 1b, which shows a range of available sizes between about 2 and 10 nm. The mean value QDs size is 4.1 nm with a standard deviation of 1.49 nm. The comparison between the two histograms suggests that the two datasets can be taken as sample cases because they show similar distribution in the available sizes of particles used to perform the experiments.

Figure 2a and b show the calculated frequencies of E_{HOMO} level evaluated in its absolute value for the data of Table 1 and Table 2, respectively. The descriptive statistics of the E_{HOMO} values are evaluated on two independent datasets and appear to be comparable since the two histograms show similar mean values equal to 5.52 eV and 5.26 eV, respectively, with standard deviations 0.35 nm and 0.40 nm, respectively.

The hypothesis is that there are correlations between the E_{HOMO}, E_{LUMO}, or ΔE with the QDs size. First, a linear model was applied to the dataset reported in Table 1. The results show that the E_{HOMO} is simultaneously influenced by both the type and size of QDs and the associated ligand. The R^2 values shown in Table 3 suggest that expecially for PbS QDs a linear correlations model can confidently be applied. The range of dimension of the QDs goes from 2 nm to 9 nm, the absolute value of E_{HOMO} ranges from 4.80 eV to 5.80 eV. All the samples show higher E_{HOMO} values for smaller sizes, as expected. The slope of the model equation, k, indicates how the size impacts on E_{HOMO} energy level. The negative values indicate that with a decrease in size an increase of the energy level is recoded, as expected from the hypothesis. All the modelled equations have slopes k ranging from −0.025 to −0.066, which suggest that the change rate of E_{HOMO} with the QDs size d is negative. All constant C values are strikingly similar regardless of the type of QDs or different ligands. Therefore, when the QD size approaches a minimal size, the E_{HOMO} will become constant regardless of what type of ligand is present (Table 3).

In Table 4, it is evaluated if there is any absolute correlation between size and HOMO energy level independently of the kind of particle considered (PbS and PbSe QDs). The linear model equation results in a R^2 value of 0.72, which confirms the hypothesis of good correlation

Table 2 E_{HOMO}, E_{LUMO}, and QD size

QDs	Capping ligand	Size, nm	LUMO, eV	HOMO, eV	Reference
CdSe	TOPO	2.3	3.76	5.77	(Amelia et al. 2011)
	TOPO	4.1	3.44	5.95	(Amelia et al. 2011)
	TOPO	4.6	3.8	5.87	(Amelia et al. 2011)
	TOPO	1.9	2.69	5.7	(Inamdar et al. 2008)
	TOPO	2.4	3.19	5.71	(Inamdar et al. 2008)
	TOPO	2.6	3.1	5.35	(Inamdar et al. 2008)
	TOPO	2.9	3.05	5.5	(Inamdar et al. 2008)
	TOPO	3.1	3.1	5.4	(Inamdar et al. 2008)
	TOPO	3.4	3.25	5.5	(Inamdar et al. 2008)
	TOPO	3.6	3.2	5.5	(Inamdar et al. 2008)
	TOPO	3.2	3.98	5.89	(Kucur et al. 2003)
	TOPO	3.5	3.96	6	(Kucur et al. 2003)
	TOPO	3.7	4.07	5.78	(Kucur et al. 2003)
	TOPO	3.8	3.66	5.6	(Kucur et al. 2003)
	TOPO	3	3.51	5.74	(Querner et al. 2005)
	TOPO	4.3	3.53	5.6	(Querner et al. 2005)
	TOPO	6.5	3.62	5.59	(Querner et al. 2005)
	TOPO	2.6	3.64	5.73	(Poznyak et al. 2004)
	TOPO	3.1	3.41	6.42	(Poznyak et al. 2004)
	TOPO	3.8	3.37	6.4	(Poznyak et al. 2004)
	TOPO	4.3	3.73	5.65	(Poznyak et al. 2004)
	1-decanethiol	2.1	−3.6	5.83	(Impellizzeri et al. 2010)
	1-decanethiol	2.3	−3.47	5.49	(Impellizzeri et al. 2010)
	1-decanethiol	2.5	−3.41	5.35	(Impellizzeri et al. 2010)
	TOPO/dithiol/Au	2.3	3.2	5.7	(Markus et al. 2009)
	TOPO/dithiol/Au	2.8	3.3	5.65	(Markus et al. 2009)
	TOPO/dithiol/Au	3.7	3.4	5.63	(Markus et al. 2009)
	TOPO/dithiol/Au	5	3.5	5.6	(Markus et al. 2009)
	TOPO/dithiol/Au	6	3.5	5.5	(Markus et al. 2009)
	2-mercaptoethanol	2	2.82	5.39	(Zhao et al. 2013)
	2-mercaptoethanol	2.3	2.93	5.47	(Zhao et al. 2013)
	2-mercaptoethanol	2.4	3.03	5.51	(Zhao et al. 2013)
	2-mercaptoethanol	2.5	3.1	5.57	(Zhao et al. 2013)
	2-mercaptoethanol	2.8	3.1	5.57	(Zhao et al. 2013)
	2-mercaptoethanol	2.9	3.14	5.68	(Zhao et al. 2013)
	2-mercaptoethanol	3	3.12	5.71	(Zhao et al. 2013)
	2-mercaptoethanol	4	3.42	5.66	(Zhao et al. 2013)
	2-mercaptoethanol	4.2	3.42	5.7	(Zhao et al. 2013)
CdTe	TOPO	3.9	3.57	5.42	(Bae et al. 2004)
	TOPO/dithiol/Au	6	–	5.1	(Wang et al. 2012)
	TOPO/dithiol/Au	5	–	5.05	(Wang et al. 2012)
	TOPO/dithiol/Au	3.8	–	5.1	(Wang et al. 2012)
	thioglycerol	2.8	–	4.88	(Poznyak et al. 2005)
	thioglycerol	3.3	–	4.98	(Poznyak et al. 2005)
	thioglycerol	3.5	–	5.01	(Poznyak et al. 2005)
	thioglycerol	3.6	–	5.03	(Poznyak et al. 2005)
	1-mercaptopropionic	2.8	–	4.93	(Poznyak et al. 2005)
	1-mercaptopropionic	3.3	–	4.95	(Poznyak et al. 2005)
	1-mercaptopropionic	3.5	–	5.03	(Poznyak et al. 2005)
	1-mercaptopropionic	3.6	–	5.08	(Poznyak et al. 2005)
PbS	oleate	2.9	3.5	–	(Hyun et al. 2008)
	oleate	3.4	3.7	–	(Hyun et al. 2008)
	oleate	4	3.9	–	(Hyun et al. 2008)
	oleate	4.8	4	–	(Hyun et al. 2008)
	oleate	5.7	4.1	–	(Hyun et al. 2008)

Table 2 (continued)

QDs	Capping ligand	Size, nm	LUMO, eV	HOMO, eV	Reference
	oleate	6.6	4.2	–	(Hyun et al. 2008)
	1-mercaptopropionic	4	3.47	–	(Sun et al. 2015)
PbSe	oleate	2	4.15	–	(Choi et al. 2009)
	oleate	3.5	4.4	–	(Choi et al. 2009)
	oleate	4	4.38	–	(Choi et al. 2009)
	oleate	4.8	4.41	–	(Choi et al. 2009)
	oleate	5.2	4.43	–	(Choi et al. 2009)
	oleate	6.5	4.58	–	(Choi et al. 2009)
	oleate	9.5	4.7	–	(Choi et al. 2009)
	oleate	4	4.27	–	(Jiang et al. 2007)
	oleate	5	4.4	–	(Jiang et al. 2007)

between the size of particles and the energy level, despite, in this case, of the differences between QDs considered. The analysis was performed also for all the other particles, but the result obtained was not good. Only for the reported ones an $R^2 > 0.5$ was found.

The same regression model was applied to the second independent dataset of Table 2: the same kind of QDs but different ligands were used in the second dataset (Table 5). Good correlation was achieved for all data collected; calculated R^2 in all cases showed values higher than 0.91, which implies high correlation between variables. It is important not to be confused by the slope obtained in this analysis: they are negative as expected, the higher value of the rate for the CdSe with 1-decanethiol ligand is due to the narrower range considered in the dimension of QDs.

The energy bandgap is a function of both E_{HOMO} and E_{LUMO} values; regression analysis was performed on E_{LUMO} energy level against the size of QDs. The results are summarized in Table 6. Good correlations are achieved for all cases with R^2 values greater than 0.78. Moreover, as expected from the hypothesis, in most cases, the E_{LUMO} level increased with the size of the QDs. Indeed the *k* values are always positive, except for CuInS2. The values are in all cases lower than unit, which means that for a unit decrease in particle size (1 nm) the energy level decreases less than one unit value (eV). A comparison was made on the energy band gap as difference between the E_{HOMO} and E_{LUMO} level against the size the QDs, by considering the different capping ligands used.

The energy band gap ΔE (eV) is equal to the difference between E_{HOMO} and E_{LUMO}, as follows:

$$\Delta E = E_{HOMO} - E_{LUMO} \tag{7}$$

Statistical analysis on the level of energy band gap ΔE is reported in Table 7. The data show good correlation against size confirming the hypothesis previously made. The R^2 value was in all cases higher than 0.5, indicating good correlation especially for CdSe QDs. The slope, *k*, index of rate of correlation, shows in all cases, except for CuInS2, negative values, which

Table 3 Correlation between HOMO energy level of first dataset (Table 1) and size of QDs

QDS	Ligand	Model	Total cases	R^2	Constant, *C*	Slope, *k*
PbS	oleate	Linear	9	0.931	5.125	−0.038
PbSe	oleate	Linear	9	0.634	5.033	−0.025
CdSe	TOPO	Linear	10	0.553	5.764	−0.066
CdTe	TOPO	Linear	8	0.683	5.143	−0.052

Table 4 Correlation between Energy of HOMO and QD size

QDS	Ligand	Model	Total cases	R^2	Constant, *C*	Slope, *k*
PbS and PbSe	oleate	Linear	18	0.720	5.071	−0.030

means that with the decrease of QDs size the energy bandgap increases. The slope, *k*, varies from −0.13 to −1.67. Therefore, the higher value of the slope shown by CdSe QDs in 1-decanethiol is due to the narrowed range of size considered, thus data available belongs to a lower array of values. Apparently, the constant *C* values are significantly different from each other, which implies that the ligands have different impact on the regression between the ΔE and QDs size.

Matlab was used to present the residuals of the regression model used in the analysis for the band gap energy values ΔE calculated using Eq. (7). Figure 3 shows the more interesting cases evaluated in terms of R^2 values and *k* values about ΔE regression analysis evaluated as size dependent variable. The graphs were divided according to the ligand used in the synthesis of the QDs.

The size of CdSe QDs can be considered as a fundamental parameter for the tunnelling of energy band gap evaluated as difference between E_{HOMO} and E_{LUMO} values. The energy band gap is also clearly influenced by organic ligands used as capping materials. Figure 4 shows that for CdSe QDs, with 1-decanethiol as capping ligand, the angular coefficient is −1.7: with low decrease in size we can notice higher decrease in band gap value with respect to the bisector 1:1. For the other ligands capping values belong to the range of −0.1 to −0.3, which means that not only achieved similar results, but confirm the hypothesis that a unit decrease in size is associated with an increase of energy band gap lower with respect to the bisector. The later observations demonstrate that size of CdSe strongly influence the energy band gap. CdS in TOPO and in TOPO/dithiol/Au has stronger capping ligands, as they show comparable size used in available data and comparable behaviour in previous regression tests. Results of simultaneous regression analysis are shown in Table 8 and Fig. 4.

Table 8 and Fig. 4 show that good correlation was achieved by the data available, with an R^2 value of 0.63. The slope of the linear regression equation, *k*, shows that a unit value decrease in size corresponds to 17% increase in energy level in the condition treated, in particular with size range between 2 and 7 nm and with selected ligands and capping.

The electronic structure of a quantum dot, strictly connected to photo-physical and chemical processes, differs from bulk sand purely molecular systems. The major reasons are the size of QDs which makes electrons quantum-confined, and the properties of the surface which defines directly the interface to the environment that surrounds the QDs. Quantum dots exhibit opto-electronic properties that are intermediate between bulk semiconductors and discrete molecules, thus they turn to be function of both size and shape (Smith and Nie 2010). QDs have sizes comparable to the de Broglie wavelength, thus the excitons result to be squeezed defining

Table 5 Correlation between the E_{HOMO} and the QD size of second dataset (Table 2)

QDS	Ligand	Model	Total cases	R^2	Constant, *C*	Slope, *k*
CdSe	1-decanethiol	Linear	3	0.945	8.317	−1.200
CdSe	TOPO/dithiol/Au	Linear	5	0.912	5.799	−0.046
CuInS2	oleate	Linear	5	0.935	6.195	−0.084

Table 6 Correlation between the E_{LUMO} and the QDs size

QDs	Ligand	Model	Total cases	R^2	Constant, *C*	Slope, *k*
CdSe	1-decanethiol	Linear	3	0.957	−4.586	0.475
CdSe	2-mercaptoethanol	Linear	9	0.946	2.373	0.258
CdSe	TOPO/dithiol/Au	Linear	5	0.893	3.062	0.080
CuInS2	oleate	Linear	5	0.939	4.812	−0.111
PbS	oleate	Linear	6	0.917	3.091	0.177
PbSe	oleate	Linear	11	0.779	4.137	0.053

quantum confinement quantified as strong, weak or intermediate, according to the difference in size (Ramirez et al. 2010). The discrete topology of the energy spectrum, mirror of opto-electronic properties of materials, is highly influenced by the confining dimension. Therefore, the band gap becomes size-dependent. The characteristic delocalization length, quantified through the "Bohr radius", is influenced by the size (Rossetti and Brus 1982; Efros and Rosen 2000). Differences in opto-electronic response arise mainly from the number of free charges (electrons and holes) and their free path (Wertheim et al. 1986). Moreover, demonstrations in correlations between polarizability and size was performed by (Ghanty and Ghosh 1993). Ionization potentials and E_{HOMO} level showed linear correlation according to (Zhang and Musgrave 2007).

Organic ligands are useful as growth surfactants and solubilizes in various media, but especially they participate in photo-physical processes that make QDs very attractive for applications such as optical sensing, fluorescent tagging, and photocatalysis. Indeed in addition to size, the modifications of surface interface by changing the molecules coordinated by the QDs lead to changes in height and shape of the potential barrier, and therefore, the degree of tunnelling of the electron and hole wave functions into the interfacial region (Harris et al. 2016; Kroupa et al. 2017). The electronic and vibrational interactions of QDs with proximate organic molecules, such as ligands, could modify the surface states, the energy and the electrons, the donors and acceptors of the QDs core and structural components. The surface ligands can stabilize the QDs geometry and prevent the formation of dangling bonds on the surface, which could otherwise act as trap states for the photo-generated carriers. The anchoring geometry of the ligand molecules plays an important role on the QDs optical properties (Azpiroz and De Angelis 2015). Passivation of the surface with organic ligands stabilizes the structure of QDs, prevents this surface relaxation, and leads to further change in absorption spectra relative to the bare QDs (Inerbaev et al. 2009).

Table 7 Correlation between ΔE in specific ligands with the QDs size

QDs	Ligand	Model	Total cases	R^2	Constant, *C*	Slope, *k*
CdSe	1-decanethiol	Linear	3	0.949	12.903	−1.675
CdSe	2-mercaptoethanol	Linear	9	0.706	2.867	−0.139
CdSe	TOPO/dithiol/Au	Linear	5	0.962	2.737	−0.127
CuInS2	oleate	Linear	5	0.676	1.383	0.027
CdSe	TOPO	Linear	7	0.645	3.489	−0.369

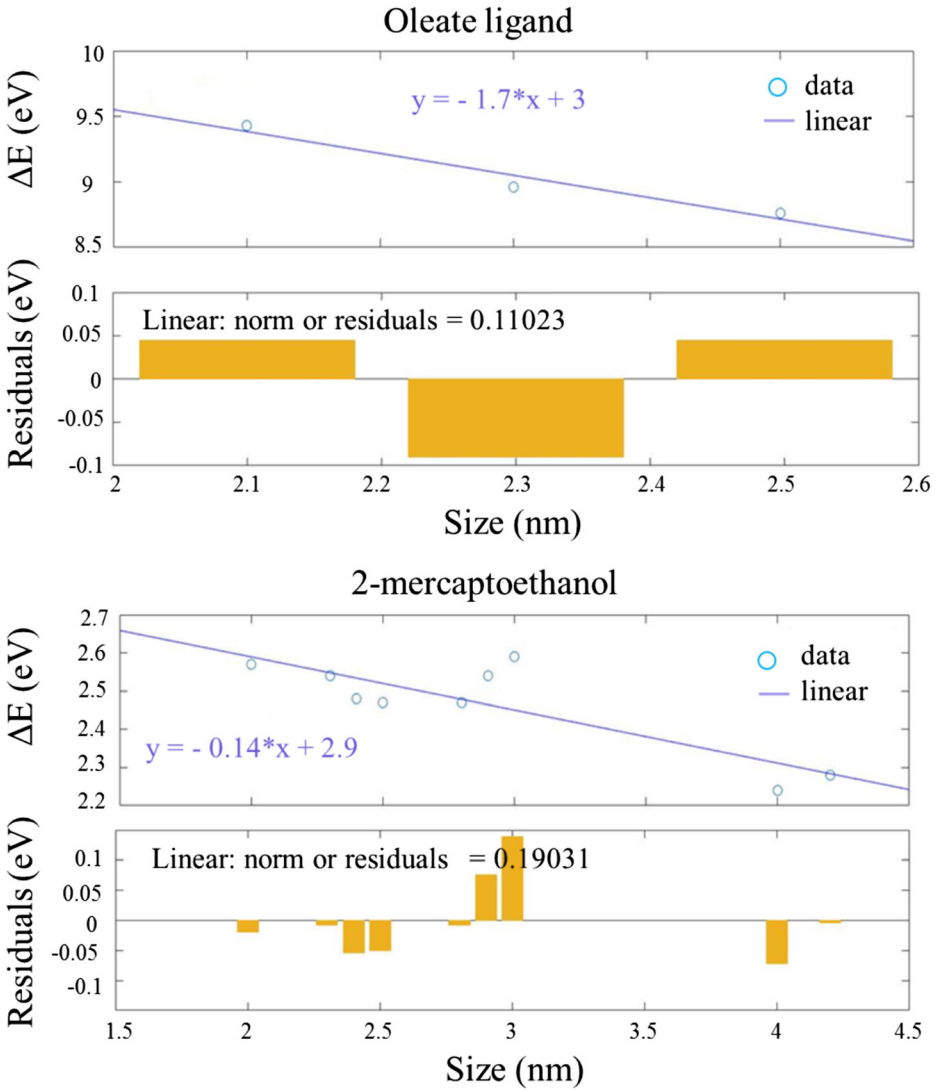

Fig. 3 Model equations and residues for regression analysis of QDs with the related ligand. From top graph to bottom: oleate; 2-mercaptoethanol; TOPO/dithiol/Au; TOPO

Changes in opto-electronic properties are linked to confinement, thus QDs size and ligand-type also affect these properties. Despite the complexity, through the manipulation of the QDs, it is possible to control the optical response and phonon-driven dynamics (Kilina et al. 2016). Therefore, many optical and electrical properties of semiconductor become function of size, for example the band gap ΔE, the absorption and fluorescence wavelengths, the ionisation potentials and electron affinities, the availability of electrons for forming bonds or getting involved in redox reactions, and thus, the catalytic activity and selectivity (Roduner 2006).

An increasing concern focusing on contaminants in the environment was registered in the past century. The methods mainly applied to eliminate pollution are physical adsorption, chemical degradation or advanced oxidation technologies. QDs are usually synthesized by

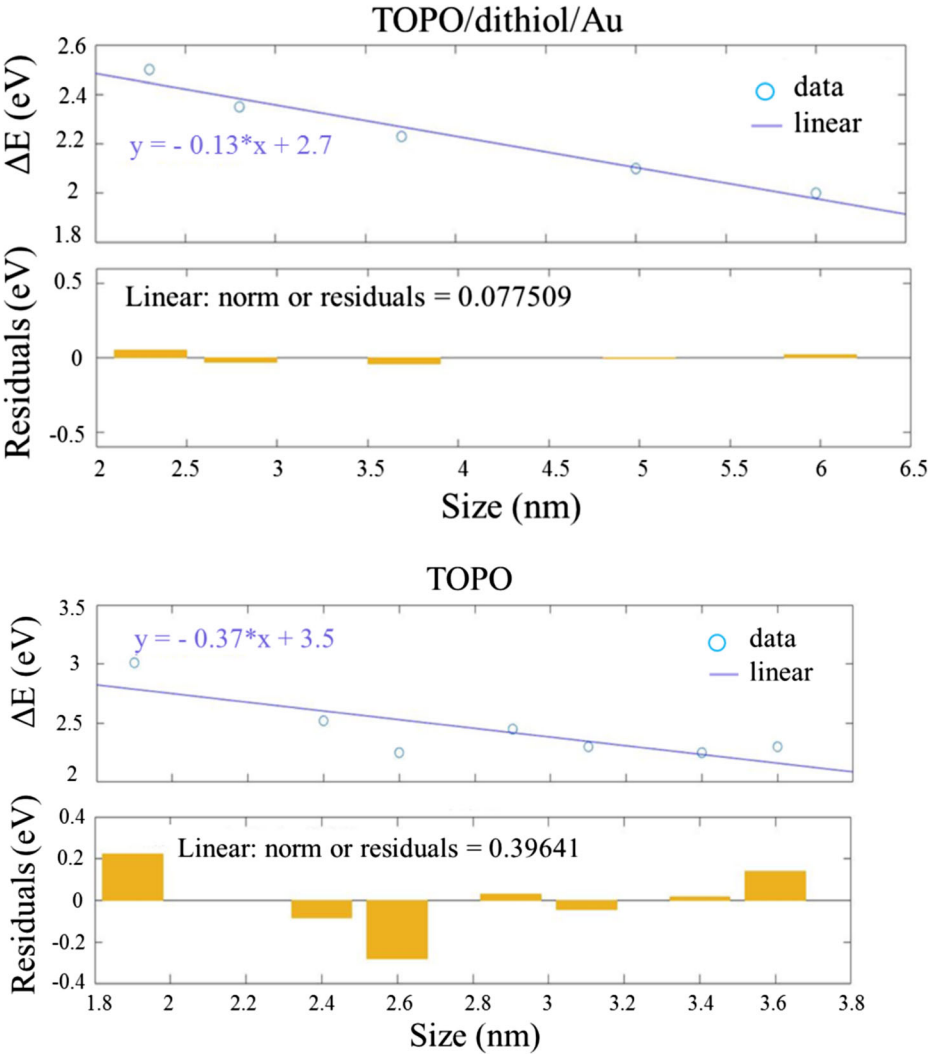

Fig. 3 (continued)

elements from II–VI (e.g., CdSe, CdTe, CdS) and III–V or IV–VI (e.g., PbSe) groups. These materials, with their rare nanometer-scale crystals, have fast become a hotspot for various applications, because of their superior optical and electro-chemical properties.

In particular, CdSe QDs were reported to be a conventional semiconductors, consisting an excellent material to apply in advanced water treatment technologies. However, this material has also some disadvantages, such as photo-corrosion or photo-dissolution, that may restrict its stability and applicability. The defects of CdSe QDs can be improved by further modification using some capping-ligands (Ma et al. 2015; Mahmoodi et al. 2016). The unique properties that make QDs

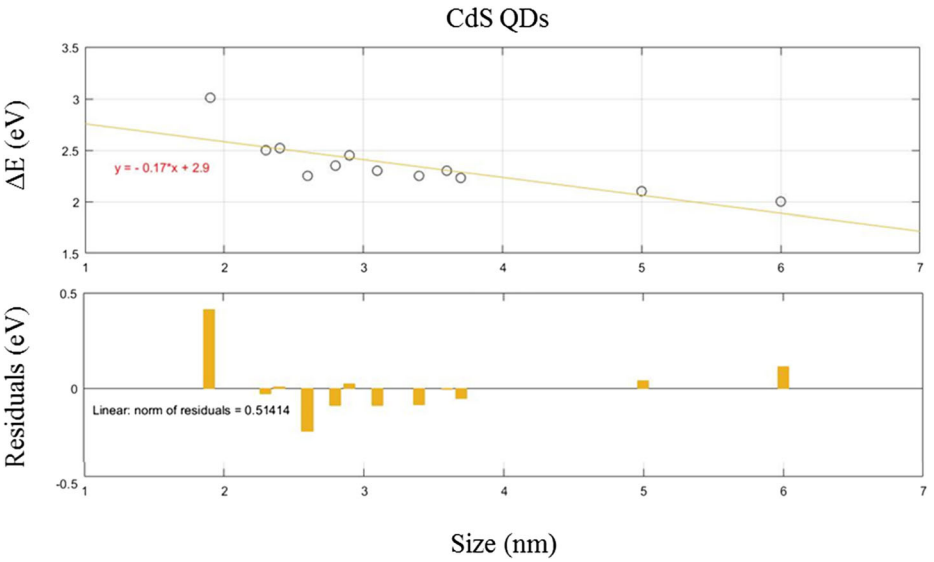

Fig. 4 Model equations and residues for regression analysis of chosen CdSe in multiple ligands

such an interesting material for wastewater treatment are strictly connected with their properties and structures. In our research, we try to correlate the morphological properties, in particular the size, to the electronic energy level for CdSe and other kind of QDs in presence of different ligands. The values considered were withdrawn from a dataset present in the literature and real case studies.

4 Conclusions

We have analyzed correlations between E_{HOMO}, E_{LUMO}, or ΔE and the QDs size in the presence of different ligands. Linear regression was found to be suitable for many of them in terms of correlation coefficient R^2, which was considered as an indicator of the goodness of model fitting. It was proved that both size and nature of organic ligand capping influence the energy levels of QDs. Optimal result was found for CdSe QDs. This class of QDs have stronger correlation between frontier molecular orbital energy levels and QDs size. The R^2 value is greater than 0.63 for a regression equation with coefficient value (slope) of −0.17 and constant 2.9. This result implies that a unit decrease of size, in a range lower than 7 nm, involves an increase in the band gap of 17%. CdSe QDs are well known as suitable materials for advanced water treatment; this is due to their tunnable optical and electronic propeties which we demonstrated in correlation to the size and surface morfology of the particles.

Table 8 Correlation between ΔE for CdSe and the QDs size in multiple lignads

QDS	Ligand	Model	Total cases	R^2	Constant, *C*	Slope, *k*
CdSe	Multiple	Linear	12	0.633	2.929	−0.174

Acknowledgements Open access funding provided by Lappeenranta University of Technology (LUT). Maa- ja vesitekniikan tuki Foundation is thanked for financial support.

References

Alivisatos AP, Gu W, Larabell C (2005) Quantum dots as cellular probes. Annu Rev Biomed Eng 7:55–76. https://doi.org/10.1146/annurev.bioeng.7.060804.100432

Amelia M, Impellizzeri S, Monaco S, Yildiz I, Silvi S, Raymo FM, Credi A (2011) Structural and size effects on the spectroscopic and redox properties of CdSe nanocrystals in solution: the role of defect states. ChemPhysChem 12:2280–2288. https://doi.org/10.1002/cphc.201100300

Azpiroz JM, De Angelis F (2015) Ligand induced spectral changes in CdSe quantum dots. ACS Appl Mater Interfaces 7:19736–19745. https://doi.org/10.1021/acsami.5b05418

Bae Y, Myung N, Bard AJ (2004) Electrochemistry and electrogenerated chemiluminescence of CdTe nanoparticles. Nano Lett 4:1153–1161. https://doi.org/10.1021/nl049516x

Bovea MD, Ibáñez-Forés V, Gallardo A, Colomer-Mendoza FJ (2010) Environmental assessment of alternative municipal solid waste management strategies. A Spanish case study. Waste Manag 30:2383–2395. https://doi.org/10.1016/j.wasman.2010.03.001

Brown PR, Kim D, Lunt RR, Zhao N, Bawendi MG, Grossman JC, Bulović V (2014) Energy level modification in lead sulfide quantum dot thin films through ligand exchange. ACS Nano 8:5863–5872. https://doi.org/10.1021/nn500897c

Brus L (2008) Noble metal nanoparticles: Plasmon electron transfer photochemistry and single-molecule Raman spectroscopy. Acc Chem Res 41:1742–1749

Burda C, Chen X, Narayanan R, El-Sayed MA (2005) Chemistry and properties of nanocrystals of different shapes. Chem Rev 105:1025–1102

Carey GH, Abdelhady AL, Ning Z, Thon SM, Bakr OM, Sargent EH (2015) Colloidal Quantum Dot Solar Cells. Chem Rev 115:12732–12763. https://doi.org/10.1021/acs.chemrev.5b00063

Choi JJ, Lim YF, Santiago-Berrios MKEB et al (2009) PbSe nanocrystal Excitonic solar cells. Nano Lett 9:3749–3755. https://doi.org/10.1021/nl901930g

Crane RA, Scott TB (2012) Nanoscale zero-valent iron: future prospects for an emerging water treatment technology. J Hazard Mater 211–212:112–125. https://doi.org/10.1016/j.jhazmat.2011.11.073

Cui Y, Wei Q, Park H, Lieber CM (2001) Nanowire nanosensors for highly sensitive and selective detection of biological and chemical species. Science 293:1289–1292. https://doi.org/10.1126/science.1062711

Dahan M, Le S, Luccardini C (2003) Diffusion dynamics of Glycine receptors revealed by single – quantum dot tracking. Science 302:2000–2003

Efros AL, Rosen M (2000) Electronic structure calculations nanocrystals. Annu Rev Mater Sci 30:475–−521. https://doi.org/10.1146/annurev.physchem.53.100301.131630

Ehamparam R, Pavlopoulos NG, Liao MW, Hill LJ, Armstrong NR, Pyun J, Saavedra SS (2015) Band edge energetics of Heterostructured Nanorods: photoemission spectroscopy and waveguide Spectroelectrochemistry of au-tipped CdSe Nanorod monolayers. ACS Nano 9:8786–8800. https://doi.org/10.1021/acsnano.5b01720

Ghanty TK, Ghosh SK (1993) Correlation between hardness, polarizability, and size of atoms, molecules, and clusters. J Phys Chem 97:4951–4953. https://doi.org/10.1021/j100121a015

Gonzalez L, Lison D, Kirsch-Volders M (2008) Genotoxicity of engineered nanomaterials: a critical review. Nanotoxicology 2:252–273. https://doi.org/10.1080/17435390802464986

Hagberg DP, Marinado T, Karlsson KM, Nonomura K, Qin P, Boschloo G, Brinck T, Hagfeldt A, Sun L (2007) Tuning the HOMO and LUMO energy levels of organic chromophores for dye sensitized solar cells. J Org Chem 72:9550–9556. https://doi.org/10.1021/jo701592x

Harris RD, Bettis Homan S, Kodaimati M, He C, Nepomnyashchii AB, Swenson NK, Lian S, Calzada R, Weiss EA (2016) Electronic processes within quantum dot-molecule complexes. Chem Rev 116:12865–12919. https://doi.org/10.1021/acs.chemrev.6b00102

Hyun B, Zhong Y, Bartnik AC et al (2008) Electron injection from colloidal PbS nanoparticles. ACS Nano 2: 2206–2212. https://doi.org/10.1021/nn800336b

Impellizzeri S, Monaco S, Yildiz I, Amelia M, Credi A, Raymo FM (2010) Structural implications on the electrochemical and spectroscopic signature of CdSe-ZnS Core−Shell quantum dots. J Phys Chem C 114: 7007–7013. https://doi.org/10.1021/jp1021032

Inamdar SN, Ingole PP, Haram SK (2008) Determination of band structure parameters and the quasi-particle gap of CdSe quantum dots by cyclic voltammetry. ChemPhysChem 9:2574–2579. https://doi.org/10.1002/cphc.200800482

Inerbaev TM, Masunov AE, Khondaker SI, Dobrinescu A, Plamadă AV, Kawazoe Y (2009) Quantum chemistry of quantum dots: effects of ligands and oxidation. J Chem Phys 131:044106. https://doi.org/10.1063/1.3135193

Jasieniak J, Califano M, Watkins SE (2011) Size-dependent valence and conduction band-edge energies of semiconductor nanocrystals. ACS Nano 5:5888–5902. https://doi.org/10.1021/nn201681s

Jiang X, Schaller RD, Lee SB, Pietryga JM, Klimov VI, Zakhidov AA (2007) PbSe nanocrystal/conducting polymer solar cells with an infrared response to 2 micron. J Mater Res 22:2204–2210. https://doi.org/10.1557/jmr.2007.0289

Kilina SV, Tamukong PK, Kilin DS (2016) Surface chemistry of semiconducting quantum dots: theoretical perspectives. Acc Chem Res 49:2127–2135. https://doi.org/10.1021/acs.accounts.6b00196

Klimov VI (2007) Spectral and dynamical properties of multiexcitons in semiconductor nanocrystals. Annu Rev Phys Chem 58:635–673. https://doi.org/10.1146/annurev.physchem.58.032806.104537

Klimov VI (2014) Multicarrier interactions in semiconductor nanocrystals in relation to the phenomena of auger recombination and carrier multiplication. Annu Rev Condens Matter Phys 5:285–316. https://doi.org/10.1146/annurev-conmatphys-031113-133900

Kroupa DM, Vörös M, Brawand NP, McNichols BW, Miller EM, Gu J, Nozik AJ, Sellinger A, Galli G, Beard MC (2017) Tuning colloidal quantum dot band edge positions through solution-phase surface chemistry modification. Nat Commun 8:2–9. https://doi.org/10.1038/ncomms15257

Kucur E, Riegler J, Urban GA, Nann T (2003) Determination of quantum confinement in CdSe nanocrystals by cyclic voltammetry. J Chem Phys 119:2333–2337. https://doi.org/10.1063/1.1582834

Liou W, Geuze HJ, Slot JW (1996) Improving structural integrity of cryosections for immunogold labeling. Histochem Cell Biol 106:41–58. https://doi.org/10.1007/BF02473201

Ma C, Liu X, Zhou M, Feng M, Wu Y, Huo P, Pan J, Shi W, Yan Y (2015) Metal ion doped CdSe quantum dots prepared by hydrothermal synthesis: enhanced photocatalytic activity and stability under visible light. Desalin Water Treat 56:37–41. https://doi.org/10.1080/19443994.2014.963152

Mahmoodi NM, Oveisi M, Arabi AM, Karimi B (2016) Cadmium selenide quantum dots: synthesis, characterization, and dye removal ability with UV irradiation. Desalin Water Treat 57:16552–16558. https://doi.org/10.1080/19443994.2015.1079259

Markus TZ, Wu M, Wang L, Waldeck DH, Oron D, Naaman R (2009) Electronic structure of CdSe nanoparticles adsorbed on Au electrodes by an organic linker: Fermi level pinning of the HOMO. J Phys Chem C 113: 14200–14206. https://doi.org/10.1021/jp9041167

Munro AM, Zacher B, Graham A, Armstrong NR (2010) Photoemission spectroscopy of tethered CdSe nanocrystals: shifts in ionization potential and local vacuum level as a function of nanocrystal capping ligand. ACS Appl Mater Interfaces 2:863–869. https://doi.org/10.1021/am900834y

Nozik AJ, Beard MC, Luther JM, Law M, Ellingson RJ, Johnson JC (2010) Semiconductor quantum dots and quantum dot arrays and applications of multiple exciton generation to third-generation photovoltaic solar cells. Chem Rev 110:6873–6890. https://doi.org/10.1021/cr900289f

Oberdörster G, Maynard A, Donaldson K, Castranova V, Fitzpatrick J, Ausman K, Carter J, Karn B, Kreyling W, Lai D, Olin S, Monteiro-Riviere N, Warheit D, Yang H, ILSI Research Foundation/Risk Science Institute Nanomaterial Toxicity Screening Working Group (2005) Principles for characterizing the potential human health effects from exposure to nanomaterials: elements of a screening strategy. Part Fibre Toxicol 2:1–35. https://doi.org/10.1186/1743-8977-2-8

Poznyak SK, Talapin DV, Shevchenko EV, Weller H (2004) Quantum dot chemiluminescence. Annu Rev Biomed Eng 4:693–698. https://doi.org/10.1021/nl049713w

Poznyak SK, Osipovich NP, Shavel A, Talapin DV, Gao M, Eychmüller A, Gaponik N (2005) Size-dependent electrochemical behavior of thiol-capped CdTe nanocrystals in aqueous solution. J Phys Chem B 109:1094–1100. https://doi.org/10.1021/jp0460801

Querner C, Reiss P, Sadki S, Zagorska M, Pron A (2005) Size and ligand effects on the electrochemical and spectroelectrochemical responses of CdSe nanocrystals. Phys Chem Chem Phys 7:3204–3209. https://doi.org/10.1039/b508268b

Ramirez HY, Lin CH, Chao CC, Hsu Y, You WT, Huang SY, Chen YT, Tseng HC, Chang WH, Lin SD, Cheng SJ (2010) Optical fine structures of highly quantized InGaAs/GaAs self-assembled quantum dots. Phys Rev B - Condens Matter Mater Phys 81:1–7. https://doi.org/10.1103/PhysRevB.81.245324

Reed MA (1986) Spatial quantization in GaAs–AlGaAs multiple quantum dots. J. Vac. Sci. Technol. B., Vol. 4, No.1, Jan/Feb 1986

Roduner E (2006) Size matters: why nanomaterials are different. Chem Soc Rev 35:583–592. https://doi.org/10.1039/b502142c

Rossetti R, Brus L (1982) Electron-hole recombination emission as a probe of surface chemistry in aqueous cadmium sulfide colloids. J Phys Chem 86:4470–4472. https://doi.org/10.1021/j100220a003

Schmalhofer WA, Calhoun J, Burrows R, Bailey T, Kohler MG, Weinglass AB, Kaczorowski GJ, Garcia ML, Koltzenburg M, Priest BT (2008) ProTx-II, a selective inhibitor of NaV1.7 sodium channels, blocks action potential propagation in nociceptors. Mol Pharmacol 74:1476–1484. https://doi.org/10.1124/mol.108.047670

Smith AM, Nie S (2010) Semiconductor nanocrystals: structure, properties, and Band Gap Engineering. Acc Chem Res 43:190–200. https://doi.org/10.1021/ar9001069.Semiconductor

Steigerwald B, Brus LE (1989) Synthesis, stabilization, and electronic structure of quantum semiconductor nanoclusters. Annu Rev Mater Sci 19:471–491. https://doi.org/10.1146/annurev.ms.19.080189.002351

Sun Z, Sitbon G, Pons T, Bakulin AA, Chen Z (2015) Reduced carrier recombination in PbS - CuInS2 quantum dot solar cells. Sci Rep 5:10626. https://doi.org/10.1038/srep10626

Wang Y, Xie Z, Gotesman G, Wang L, Bloom BP, Markus TZ, Oron D, Naaman R, Waldeck DH (2012) Determination of the electronic energetics of CdTe nanoparticle assemblies on au electrodes by photoemission, electrochemical, and photocurrent studies. J Phys Chem C 116:17464–17472. https://doi.org/10.1021/jp306702t

Wertheim GK, DiCenzo SB, Buchanan DNE (1986) Noble and transition-metal clusters: the d bands of silver and palladium. Phys Rev B 33:5384–5390. https://doi.org/10.1103/PhysRevB.33.5384

Yadav KK, Singh JK, Gupta N, Kumar V (2017) A review of nanobioremediation technologies for environmental cleanup: a novel biological approach. J Mater Environ Sci 8:740–757

Yin JJ, Lao F, Fu PP, Wamer WG, Zhao Y, Wang PC, Qiu Y, Sun B, Xing G, Dong J, Liang XJ, Chen C (2009) The scavenging of reactive oxygen species and the potential for cell protection by functionalized fullerene materials. Biomaterials 30:611–621. https://doi.org/10.1016/j.biomaterials.2008.09.061

Yoshizawa K (2012) An orbital rule for electron transport in molecules. Acc Chem Res 45:1612–1621. https://doi.org/10.1021/ar300075f

Yu WW, Chang E, Falkner JC, Zhang J, al-Somali AM, Sayes CM, Johns J, Drezek R, Colvin VL (2007) Forming biocompatible and nonaggregated nanocrystals in water using amphiphilic polymers. J Am Chem Soc 129:2871–2879. https://doi.org/10.1021/ja067184n

Zhang JZ (1997) Ultrafast studies of electron dynamics in semiconductor and metal colloidal nanoparticles: effects of size and surface. Acc Chem Res 30:423–429. https://doi.org/10.1021/ar960178j

Zhang G, Musgrave CB (2007) Comparison of DFT methods for molecular orbital eigenvalue calculations. J Phys Chem A 111:1554–1561. https://doi.org/10.1021/jp061633o

Zhang J, Nazarenko Y, Zhang L, Calderon L, Lee KB, Garfunkel E, Schwander S, Tetley TD, Chung KF, Porter AE, Ryan M, Kipen H, Lioy PJ, Mainelis G (2013) Impacts of a nanosized ceria additive on diesel engine emissions of particulate and gaseous pollutants. Environ Sci Technol 47:13077–13085. https://doi.org/10.1021/es402140u

Zhao J, Holmes MA, Osterloh FE (2013) Quantum confinement controls photocatalysis: a free energy analysis for photocatalytic proton reduction at CdSe nanocrystals. ACS Nano 7:4316–4325. https://doi.org/10.1021/nn400826h